Chapter 5
The Reproduction of the Physiological Behaviour of the Axon of Nervous Cells by Means of Finite Element Models

Simona Elia and Patrizia Lamberti

Dept. of Electronic and Computer Engineering, University of Salerno, Italy
{selia,plamberti}@unisa.it

Abstract. This paper describes 3D Finite Element modelling solutions for a segment of a nervous cell axon, which take into account the non linear and time varying dynamics of the membrane surrounding it in order to reproduce its physiological behaviour, in terms of Action Potentials (AP) elicitation and its temperature dependence. The axial-symmetry of the system is exploited in order to conduct a more efficient analysis. A combination of the so called Hodgkin-Huxley equations modelling the dynamics of the membrane voltage-controlled ionic channels, together with the Maxwell equations in Electro Quasi-Static approximation, describing the electromagnetic behaviour of each medium, is tackled in a numerical procedure implemented in a commercial Finite Elements multiphysical environment. The usefulness of Finite Elements in order to have interesting quantitative responses (field shape and axon physiological behaviour) is investigated. Two different models are presented here. One exploits the typical thin layer approximation for the axon membrane, proving to be useful when the field solution inside the membrane domain is not a matter of interest. Its performances are compared with the other model, which is introduced in order to obtain a more realistic representation of the studied system: the axon membrane is here realized with a non-linear active medium (exploiting its equivalent electric conductivity) allowing the reproduction of the electric potential also inside the membrane. The passive electrotonic nature of the membrane and the elicitation of an AP in presence of different stimuli are computed and the results are in keeping with the predicted ones. Finally the AP temperature dependences and the propagation effect are reproduced by using the corresponding "best" numerical model, i.e. the coarse one without membrane for the temperature, the more detailed with membrane for the propagation, leading to a trade off between the computational effort and the objective of the analysis. The models open a wide range of applications and extensions in order to understand the true behaviour of a complete neuron.

Keywords: Axon, Neuron, Hodgkin-Huxley equations, FEM.

Introduction

Computational modelling and analysis in biology and medicine have received major attention in recent years in order to understand, analyze and predict the complex

I. Jordanov and L.C. Jain (Eds.): Innovations in Intelligent Machines -3, SCI 442, pp. 69–87.
springerlink.com

mechanisms of biological systems [1]-[3]. Neural prosthetics can considerably widen the lifespan and health quality of people and thus the mechanisms of neuron firing and transmission of signals are increasingly investigated [1]. In order to study the influence of electrical signals on the nervous cells for setting appropriate stimulation protocols and to design efficient equipment, proper models are needed, capable of describing the phenomena occurring at the interface between neural cells and stimulating electrodes [4]-[7].

In order to obtain a model able to predict cell response phenomena the nearest possible to the reality when they are "artificially" induced by external stresses, the first step is to test its capability to reproduce the "natural" phenomena. i.e. the physiological behaviour of the axon. In this paper a realistic cylindrical shaped segment of a nervous cell axon (the neuronal structure carrying nervous signals) is considered. Its electromagnetic physiological behaviour, at different temperatures, is studied by using two alternative 3D models, both implemented exploiting the Finite Element Method (FEM) in axial-symmetry for the solution of the Maxwell Equation in its Electro Quasi Static (EQS) formulation, coupled with the so called Hodgkin-Huxley (HH) equations [8]. This problem is typically studied by using compartmental models for the axon behaviour ([9]-[11]) and solved by means of the cable theory that doesn't furnish the shape of the electromagnetic field around and inside the axon. As a consequence a direct quantitative study of the interaction of the neuron with the applied electric stimulus, the dependences of the responses on the geometric features of the electrode and the influence of the electromagnetic characteristics of the external medium are not easy to obtain or also sometimes even impossible to achieve. Vice versa a "field solution" of the problem leads to the availability, for example, of the voltage profile inside all the modelled domain [12]. Therefore it can be useful, in order to understand the interaction of the axon with other neighbouring structures, such as another neuron. In that case some interesting results can be obtained, capable to take in to account, for example, the ephaptic effect among axon fibers or between them and somas or dendrites [13]. To this aim, the lumped-circuit quantities of the HH electrophysiological model can be transformed into parameters adapt to an electromagnetic field solution study, as in [14]. Thus here, the EQS formulation of the Maxwell equations, describing the relevant phenomena, is faced and the non linear differential equations describing the membrane behaviour are efficiently and accurately combined with the FEM solution in a numerical procedure performed by using a commercial software (COMSOL Multiphysics®), implementing their effects by means of opportune outward normal current densities on the boundary. This approach leads to a coarse FEM model of the axon that, by exploiting the concept of thin-layer approximation, is useful and computationally efficient when the field solution inside the membrane domain is not matter of interest. Moreover the possibility to model the axon membrane is also considered here: the axon membrane domain is instead realized with a non-linear active medium (exploiting its equivalent electric conductivity) in order to obtain a more realistic model of the axon. This approach leads to a different FEM model of the axon allowing the reproduction of the electric potential also inside the membrane. This way, the electric potential and its variation along all the modelled region is given with a corresponding computational cost, lower for the first model, higher for the second one. A comparison of the two models is performed in order to assure their coherence with literature specific

behaviour as it concerns the correct reproduction of the passive membrane electrotonic response and the elicitation of APs in presence of different stimuli. In this paper, to assure the solution the ability to reproduce the physiological behaviour at different environmental conditions, as experimentally found by HH, the temperature-dependency of the voltage-controlled ionic channels is also introduced in our FEM models, as reported by HH [15]-[17], to accurately describe channels activation/ inactivation properties. The efficiency of the FEM approach with respect to variation in the quality of the numerical solution is performed by comparing the predicted behaviour with respect to the experimental one given in [17]. Finally the AP temperature dependences and the propagation effect are reproduced by using the corresponding "best" numerical model, i.e. the coarse one without membrane domain analysis in temperature, the more detailed with membrane for the reproducing propagation phenomenon, leading to a trade off between the computational effort and the objective of the analysis. Due to their simple implementation, the proposed models can be easily used to simulate the behaviour of more complex nervous structures. The paper is organized as follows: in Section 1 the two alternative model are introduced starting from the more realistic one (Model A), that reproduces the presence of the membrane; it is, then, followed by the introduction of the coarse one (Model B), that is obtained by considering the thin-layer approximation of the membrane domain. Here a comparison between the two models is conduced with respect to assigned input current, leading to assure the capability of both models to reproduce the electrotonic behaviour and the AP elicitation. The Section 2 is dedicated to the introduction of the temperature dependency in the physics of the membrane and used to test the capability of a FEM approach to predict the behaviour with respect to variation in its "numerical" quality. Finally in the Section 3 the AP temperature dependences and the propagation effect are reproduced by using the corresponding "best" numerical model, leading to the conclusion reported at the end of the paper and opening a wide range of future work, there indicated too.

1 Proposed FEM Axon Models

The schematic structure of an axon segment of nerve cell surrounded by its membrane (or axolemma) is pictured in Figure 1.

It is a tubular shaped structure, delimited by three cylindrical surfaces, to delimitate three different domains: the axoplasm, the axolemma and the extracellular domain. The first one is the internal part of the neuron consisting of cytosol, the second one, which is representative of the membrane of the axon, is the domain in which the exchange of ionic charges (Na^+, K^+ and leakage) determines the active electromagnetic behaviour of the neuron and it is delimited between the two first coaxial cylindrical surfaces with a very thin thickness (~nm); in the end, the third domain, representing the external medium in which the neuron is immersed, characterized by electromagnetic properties similar to the first domain, is delimited by the second and third coaxial cylindrical surfaces, with a thickness of the order of the micron. Due to the evident axial symmetry, the three dimensional axon segment of the nerve cell can be studied by considering only the pink-highlighted two dimensional section in Figure 1 and by modelling the system in a cylindrical coordinates system. It

is thus possible to pass from the three 3D domains represented in Figure 1 to the three 2D rectangular domains in the more realistic model (i.e. Model A, reported in Figure 2a) or the two 2D rectangular domains divided by a discontinuity boundary in the computationally-reduced model (i.e. Model B, reported in Figure 2b), in which the thin layer approximation of the membrane domain is used [18].

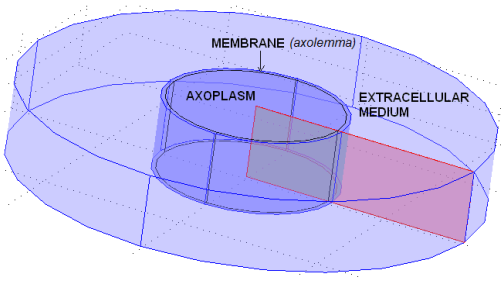

Fig. 1. The axon slice under analysis (3D sketch). The section in r-z plane is highlighted in pink.

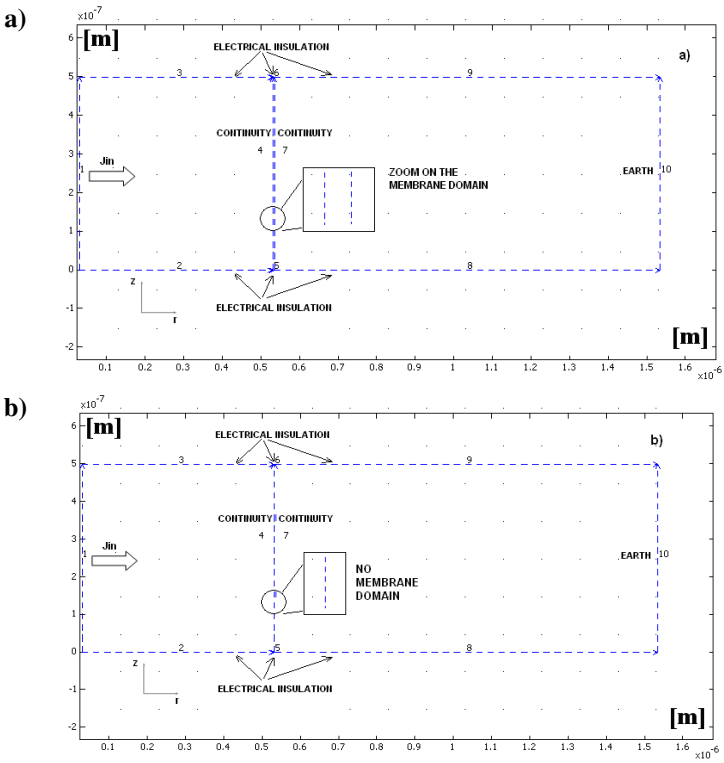

Fig. 2. Axial-symmetric 2D section in r-z plane, with boundary conditions chosen: a) Model A; b) Model

1.1 Model A – Axon with Membrane Domain

The basic geometry used to model the axon, in this case, is reported in Figure 2a. In particular, we model a section of $1.505\times0.5\mu m^2$ ($0.5\mu m\times0.5\mu m$ for the axon domain, D_a, $5nm\times0.5\mu m$ for the membrane domain, D_m, and $1\mu m\times0.5\mu m$ for the external medium represented by D_e). The small size of the system with respect to the characteristic wavelength of the typical electromagnetic fields over the whole structure and the low contribution of the energy associated to the magnetic field compared to that stored in the electric field allow the adoption of the Electro QuasiStatic (EQS) approximation of Maxwell equations. Therefore on this geometry the physiological behaviour of the whole system is obtained by using the 2D axial symmetric transient analysis set of equation of the Quasi-Static Electric AC/DC module, the time dependent analysis of the Partial Differential Equation (PDE) mode and the extrusion tool, offered by the adopted software environment: COMSOL Multiphysics. Sub-domains D_a and D_e are implemented as linear, homogeneous and isotropic dielectric materials, described by their constant electric conductivity, σ_a and σ_e, and dielectric permeability, ε_a and ε_e respectively. The corresponding values are reported in Table 1. On D_m, besides a constant permittivity ε_m, a non linear equivalent conductivity σ_m defined by (2) and an external current density depending on the voltage across the membrane are used in order to approximate the nonlinear behaviour of the medium with respect to the imposed electric field (according to the HH model of the membrane). In particular, HH circuit-equations must be "converted" to obtain their electromagnetic *field equivalent* [19].

First of all, since membrane thickness is very small, it can be looked at as a parallel plate capacitor. Therefore its dielectric and equivalent conductivity can be derived from values found in literature [8]. In particular, once defined all the constant parameters as in Table 1, the dielectric constant per unit area is

$$\varepsilon_m = \frac{C_m d_m}{\varepsilon_0} \tag{1}$$

whereas membrane equivalent conductivity σ_m can be derived by HH overall membrane conductance, G_m, defined as a function of the Sodium (Na), Potassium (K) and Leakage conductances (l) [16] and depending on transmembrane voltage (TMV) through the so called channel activation variables. Then, σ_m becomes:

$$\sigma_m = G_m \cdot d_m \tag{2}$$

where

$$G_m = \sum_i G_i \quad \text{with } i \in \{Na, K, l\} \tag{3}$$

Table 1. Parameters appearing in the model

Parameter	Value	Description
ε_m	5.65	Membrane relative dielectric constant
C_m [μF/cm^2]	1	Membrane capacitance per unit area
d_m [nm]	5	Membrane thickness
G_{Namax} [mS/cm^2]	120	Conductance per unit area of the Na channel
G_{Kmax} [mS/cm^2]	36	Conductance per unit area of the K channel
G_l [mS/cm^2]	0.3	Conductance per unit area of the leakage channels
E_{Na} [mV]	55	Nernst voltage due the Na concentration
E_K [mV]	-72	Nernst voltage due the K concentration
E_l [mV]	-49.38	Nernst voltage due other ionic concentrations
σ_{Ax} [S/m]	0.5	Axoplasm conductivity
ε_{Ax}	80	Axoplasm dielectric constant
σ_{Ext} [S/m]	1	External medium conductivity.
ε_{Ext}	80	External medium dielectric constant

The expressions of ionic channel conductances, reported in (4.a) and (4.b) show their connection with the activation/inactivation variables m, n and h, implicitly defined by the differential equations set (5):

$$G_{Na} = G_{Na\max} m^3 h \tag{4.a}$$

$$G_K = G_{K\,max} n^4 \tag{4.b}$$

$$\frac{dx}{dt} = \alpha_x \cdot (1 - x) - \beta_x \cdot x \tag{5}$$

where $x \in \{m,n,h\}$.

The transfer rate coefficients α_x, β_x, in (5), are not constant numbers but, as shown in Table 2, depend on the value of the voltage across the axon membrane – the so-called transmembrane voltage, TMV here defined as $V_m(x,y,z,t)=V_m(r,\phi,z,t) = V_m(r,z,t)$ – through V', which represents the TMV deviation from the resting value V_{stat}=-60mV.

Table 2. Expressions of the transfer rate coefficients and corresponding initial values [1/s]

	α_x		β_x	
x	**expression**	**initial value**	**expression**	**initial value**
n	$1000\frac{0.1-0.01V'}{e^{(1-0.1V')}-1}$	*58.19*	$1000\frac{0.125}{e^{0.0125V'}}$	*125*
m	$1000\frac{2.5-0.1V'}{e^{(2.5-0.1V')}-1}$	*223.56*	$1000\frac{4}{e^{(V'/18)}}$	*4000*
h	$1000\frac{0.07}{e^{0.05V'}}$	*70*	$1000\frac{1}{e^{(3-0.1V')}+1}$	*47.42*

The HH trans-membrane current density equation for a unit area patch of membrane can be expressed as:

$$I_m = C_m \frac{dV_m}{dt} + \sum_i (V_m - E_i) G_i \quad \text{with } i \in \{Na, K, l\} \tag{6a}$$

Separating the term depending on V_m and the one depending on the Nernst potentials, I_m becomes

$$I_m = C_m \frac{dV_m}{dt} + V_m \sum_i G_i - \sum_i E_i G_i = C_m \frac{dV_m}{dt} + V_m G_m - J_e \tag{6b}$$

with $i \in \{Na,K,l\}$. J_e is modeled as an externally impressed current, taking into account the Nernst potential, and is defined as

$$J_e = \sum_i E_i G_i \quad \text{with } i \in \{Na, K, l\} \tag{7}$$

Furthermore, the equation of continuity implemented everywhere over the FEM model can be written as

$$\nabla \cdot \frac{\partial(\varepsilon_i \nabla V)}{\partial t} + \nabla \cdot (\sigma_i \nabla V - \bar{J}_{ext}) = 0 \tag{8}$$

where

$$\bar{\mathrm{J}}_{\mathrm{ext}} = \begin{cases} 0 & \text{over } \mathrm{D_a} \cup \mathrm{D_e} \\ Je \cdot \hat{r} & \text{over } \mathrm{D_m} \end{cases} \tag{9}$$

The continuity equation (8) must be implemented on the whole model, whereas the HH equations system is associated only to the membrane domain $\mathrm{D_m}$. As the three voltage-controlled conductances G_{Na}, G_K and G_l are meaningful *only on membrane domain* and not externally, they require to be *only locally* defined. The flexibility of COMSOL Multiphysics® proves useful in handling variables, as well as in the post-processing phase. In the simulation session a set of *PDEs* is coupled to the Electrostatic module: the first one is employed in order to solve equation (8) with respect to the so-called dependent variable (in this case *electric potential*, *V*), whereas the second one is introduced to solve the three differential equations in *m, n, h (dependent variables)*, representing channel activation variables according to the HH model ([8]), as shown in the equations reported in system (5).

In order to obtain the voltage values along both sides of membrane, point by point along the z coordinate, the "extrusion" feature is conveniently employed. n fact, the equations implemented there, explicitly depend on TMV, $V_m(r,z\,t)$:

$$V_m(r,z,t) = V_i(r,z,t) - V_o(r,z,t) \tag{10}$$

where V_i and V_o are the voltage across the boundaries 4 and 6, respectively (Figure 2a). This way the HH lumped-circuit quantities are "translated" into parameters adapt to a field solution study, as previously highlighted. It must also be noticed that, while ε_m obtained is a constant, σ_m depends on $V_m(r,z,t)$.

1.2 Model B – Axon with Thin Layer Approximation

The basic geometry used to model the axon in this case is reported in Figure 2b. In particular, we model a section of $1.5\times0.5\mu m^2$ ($0.5\mu m\times0.5\mu m$ for the axon domain, D_a, and $1\mu m\times0.5\mu m$ for the external medium represented by D_e). Also in this case, the physiological behaviour of the whole system is obtained by using the 2D axial symmetric transient analysis packet of the Quasi-Static Electric AC/DC module whereas the time dependent analysis of the PDE mode packet adopted is in weak form and the possibility to perform a thin layer approximation ([18]) is exploited in order to have a computationally less costly model, as in [14]. In fact, the cell membrane is an extremely thin structure that increases the simulation time and memory request in FEM. This applies to the short axon segment under analysis and it is especially true in the perspective of a generalization of the model to a whole axon. Indeed, if it were necessary to simulate the behaviour of a very long neuron (i.e. a motoneuron), this would result in a form factor (length of the axon divided by membrane thickness) that could also be of the order of 10^9. In order to simplify meshing and to greatly reduce simulation time and memory request it is useful to employ a thin layer approximation for the membrane. It is, thus, possible to completely avoid the physical realization of the corresponding thin domain, by substituting it, with an interface surface. This leads to an alternative model, B (Figure 2b), that completely satisfies the hypotheses of applicability of the approximation:

1) there is a substantial difference between membrane domain conductivity and those of the other two domains;

2) lateral boundaries are insulated (null net flux);

3) current density components along ϕ and z are negligible with respect to that along r-axis.

In particular, it is possible to approximate the potential distribution along the membrane thickness as being linearly varying from V_o to V_i. Thus, by using the continuity equation for the current, it is easy to derive the expression for an equivalent current density J_{eq} [14]:

$$J_{eq} = \sigma_m \frac{(V_2 - V_1)}{d_m} + J_e + \frac{\varepsilon_m \varepsilon_0}{d_m} \frac{\partial (V_2 - V_1)}{\partial t} \tag{11}$$

where V_1 and V_2 represent the voltage values along the membrane boundaries 4 and 7 of Figure 2, respectively. This equation can be implemented by using two different Electrostatics packets in order to allow the solver to "see" interface surface (substituting the membrane domain of the model A) once as belonging to axoplasm D_a and once to the external medium domain D_e. It is clearly expectable that voltage on that boundary will have a discontinuity (V_2-V_1) almost equal to the value that the TMV would have reached, if the membrane were really implemented in the model as a 2D domain. Thus, V_1 is set as an *active* variable only in the axoplasm domain, V_2 only on the external medium domain, while both are defined on their interface. J_{eq} is imposed as an input current density on this boundary, as in [14]. In addition, an alternative formulation of the three non linear differential equations reported in (5) must be provided on this surface where all expressions are locally defined. The idea is to substitute the *PDE*s formulation, adopted in the version A of the model, with its

weak formulation (for boundaries). This choice allows to handle all the equations in the integral form, multiplying both sides of each equation by a test function and then integrating.

1.3 Model A vs. Model B

In order to make a fair comparison between the two modelling solutions, some FEM common parameters are adopted as reported in Table 3.

Table 3. Parameters used for comparing the two models

Calculus and mesh parameters	Value
Simulation times [s]	$0{:}10^{-4}{:}0.02$
Relative tolerance	10^{-4}
Absolute tolerance	10^{-8}
Max. element size scaling factor	1
Element growth rate	1.3
Mesh curvature factor	0.3
Mesh curvature cut off	0.001

The same initial and boundary conditions are fixed everywhere, exception made for the various settings related to membrane domain, since it is not present in the Model B. This settings induce the meshes pictured in Figure 3 in which the increase is evident in the number of elements due to the presence of a thin structure, represented by the membrane domain in the Model A (Figure 3a), if compared with the Model B (Figure 3b).

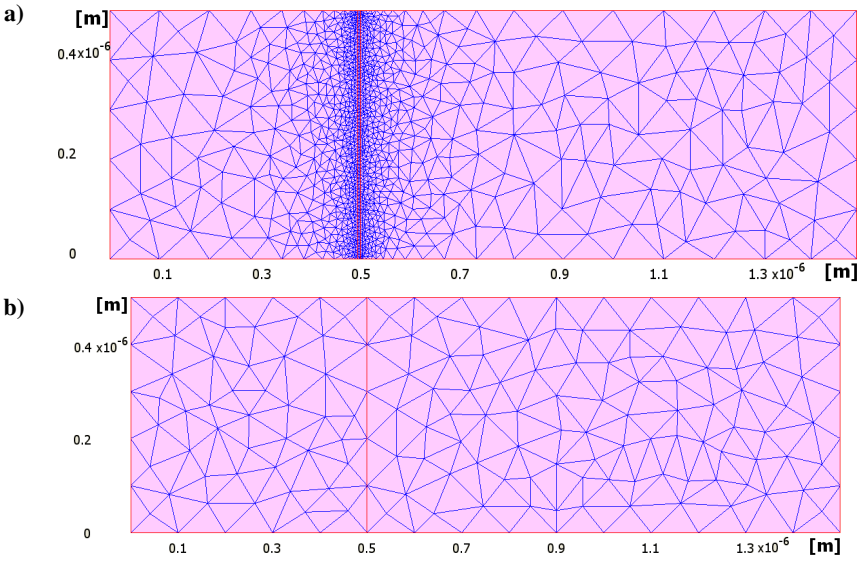

Fig. 3. Meshed 2D geometry: a) model A with membrane, b) Model B without membrane

The simulation is carried out, by fixing all initial conditions from nominal resting values. The iterative procedure is stopped when the numerical variations are *sufficiently* negligible leading to the "equilibrium" steady state conditions. This condition is adopted as a starting point for studying the cellular responses elicitation by applying a square window current density stimuli of different amplitude and duration to boundary 1 (Figure 2). In Table 4 the degrees of freedom and the number of elements for the two different models are reported together with the simulation duration, necessary to achieve equilibrium (the stable stationary condition for the neuron at rest).

Table 4. Figures of merit concerning the two FEM models and corresponding simulation time

PARAMETER/MODEL	A	B
Degrees of freedom	7086	685
Number of elements	2378	300
Simulation duration for the equilibrium state	13.00 s	2.63 s

By looking at the Table 4, the difference is evident of almost one order of magnitude for the considered figures of merit, concerning the more detailed FEM Model A with respect to the coarse one (Model B), leading to a five times larger simulation time for the reproduction of the axon behaviour for the adoption of the first model. In Table 5, instead, the case of 20ms of membrane behaviour simulation is reported when it undergoes a stimulus-induced response. The considered current stimulus is given by 4 rectangular shape obtained by combining a short-d (2ms) or long-D (19ms) duration and low-m (0.03A/m^2) or high-M (0.3 A/m^2) magnitude.

Table 5. Simulation times (in [s]) for the computation of 20ms of membrane behaviour

	d/m	d/M	D/m	D/M
Model A	83.64	185.59	119.31	183.71
Model B	19.79	48.96	26.89	42.70

In this case an appropriate current density (J_{in}, the square window shown in the Inset of Figure 4a) is applied at $r=r_1$=1nm, very close to the symmetry axis, in order to trigger the excitable membrane (if current density stimulus where injected exactly at r=0μm, current density would have been undefined). A great advantage is offered by Model B in the dynamic case too, as far as stimulation length is concerned. Indeed, for all the considered stimuli, in order to obtain the time shape of the TMV in a time window of 20ms, a simulation time is found of also more then 3' for the Model A, with respect to almost 40 s for the Model B, as reported in Table V. In Figure 4, the membrane responses obtained at r=0.6μm z=0.2μm for the Model A (blue curves) and Model B (red curves) for each considered case are depicted.

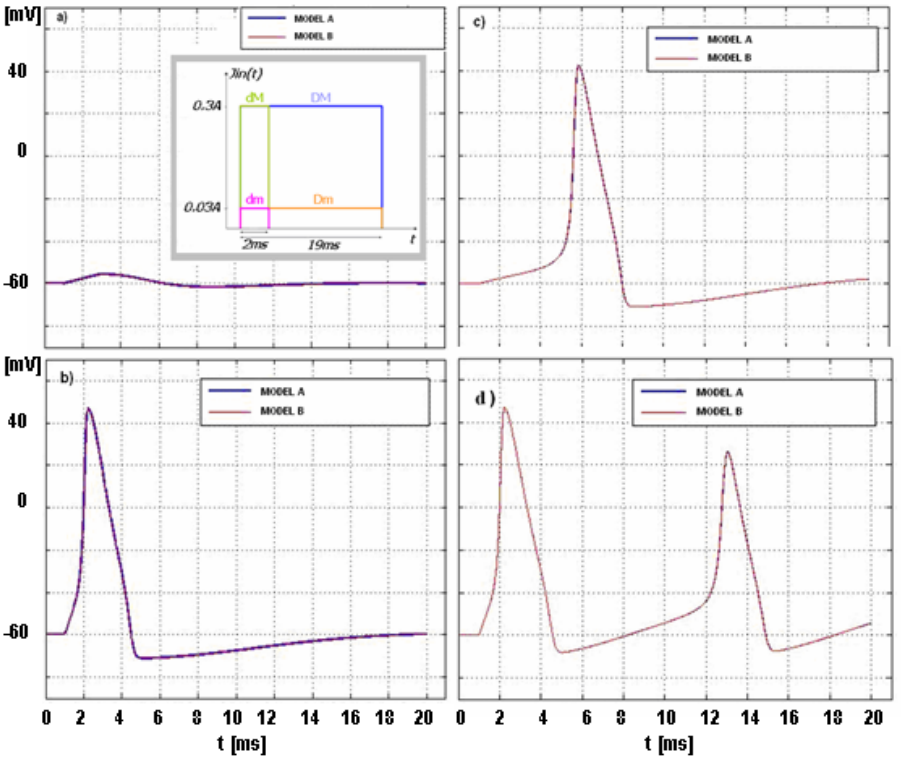

Fig. 4. Membrane response in terms of $V_m(0.6\mu m,0.2\mu m,t)$: a) *dm*, b) *dM, c) Dm*, d) *DM*. Inset: Input stimulus parameters

In order to compare the two models, the relative difference between the maximum value reached by the AP, obtained by means of Model A with respect to that of Model B is used (the value calculated with Model A is considered as reference value due to the fact that it comes from the more realistic model). The behaviours obtained with both the models are totally in accordance with theoretical expectations [20]. As reported in Figure 4a, in the first case (*dm*) the stimulus is not sufficient to elicit any AP (sub-threshold behaviour, whose parameters, rise time and amplitude, are those expected) showing a passive electrotonic nature of the membrane, being it approachable (at least in first approximation) as an R-C circuit. The relative error between the two models is computed as 0.04%. In the second and in the third cases (see Figures 4b and 4c), an AP is observed (relative error 0.01% and 0.05% respectively), while in the fourth one, since both strength and duration of the stimulus pulse are high (see [7],[20]), two APs are excited, the second of which is lower than the other, because refractory period is not respected. In this last case, depicted in Figure 4d, the relative error is the same as in the case a), i.e. 0.01%, as it is expected due to the fact that the input is the same at the time instant in which the maximum TMV value is reached. It is interesting to observe how membrane responses, in the four corresponding cases almost coincide in the two modelling approaches, with a

relative variation not higher then 0.05%. Therefore the coarse Model B seems to be a very good representation of the reality if compared with the fine Model A and the best choice in terms of computational effort. Actually the Model A furnishes the voltage profile along the *r* direction all over the structure considered for the 3D axon sketch (Figure 1), whereas in the Model B no information is available for the axolemma membrane. Therefore, in presence of a lower computational effort, the adoption of the Model B can be conveniently considered in order to evaluate phenomena external to the membrane domain, otherwise the "more realistic" Model A must be adopted.

2 AP Temperature Dependence and Feature of a FEM Approach

The simulations described in the previous section are carried out supposing an operation temperature of 6.3°C, such as the one used by HH in their measurement phase [8] and simulated in [20], with respect to the same current input stresses. Moreover, the channels conductances exhibit a time behaviour that is described by an opportune time constant and that is governed by the activation/inactivation of the corresponding ionic species. The temperature dependency of the gating process, according to [15], can be described by:

$$\frac{dx}{dt} = \left[\alpha_x (1-x) - \beta_x x\right] \cdot 3^{\frac{T-6.3}{10}} \tag{12}$$

with $x \in \{m,n,h\}$. This yields to:

$$\frac{dx}{dt} = \left[\alpha'_x (1-x) - \beta'_x x\right] \tag{13}$$

leading the original rate coefficients reported in Table 2 to change into α'_x and β'_x thanks to the introduction of the temperature-dependent factor $3^{(0.1T-0.63)}$. The time constant τ_x of the "channel-gating" processes results scaled of the same factor leading to a faster dynamic:

$$\tau'_x = \frac{1}{\alpha'_x + \beta'_x} = \frac{\tau_x}{3^{\frac{T-6.3}{10}}} \tag{14}$$

Adding also temperature dependence to the model, i.e. using the new transfer rate coefficients in the FEM Model A and B, it is easy to obtain the TMV for temperatures within the theoretical validity range of the HH model ([11],[21]). Nevertheless, as far as the interest is on the capability of the FEM approach to reproduce the temperature dependency not necessary in the membrane domain, the behaviour of the TMV with respect to that for only the coarse model (Model B) is performed. In particular, by considering the same temperature experiment performed and theoretically predicted by HH in [17], the obtained time shape of the TMV is reported in Figure 5, showing a good reproduction of the results.

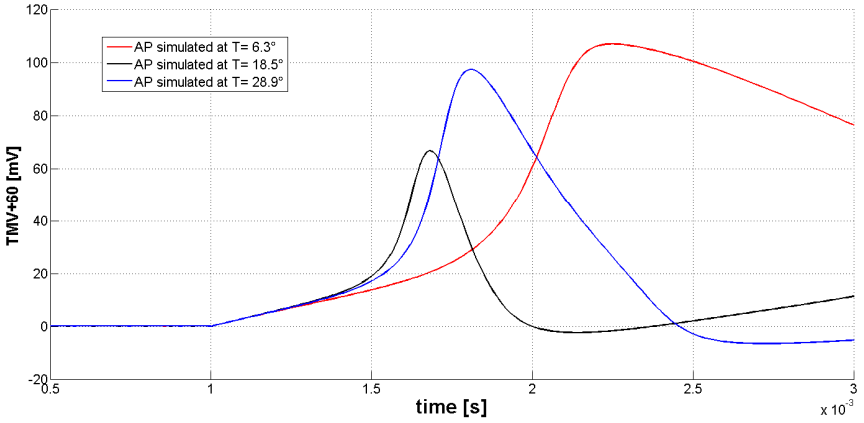

Fig. 5. Simulated TMV behaviour as in [17], obtained with the FEM-Model A

In order to assure the reliability of the FEM solution in terms of the quality of the numerical approximation of the "actual behaviour", i.e. the experimental one, in Table 6 a comparison is reported on the TMV maximum value estimation between a base meshing of the geometry and a more refined one.

Table 6. Comparison of the mesh-cost vs accuracy of the predicted data

PARAMETER/MODEL	Base Mesh	Refined Mesh
Degrees of freedom	7086	27280
Number of elements	2378	9512
Simulation duration	13.00 s	133s
Relative error @T=6.3°C	-1.4312%	-1.4313%
Relative error @ T=18.5°C	-1.6730%	-1.6735%
Relative error @ T=28.9°C	-10.4043%	-10.4045%

In particular, by increasing the approximation of the geometry with a mesh-refinement, an increase on the computational cost in terms of simulation times of a factor ten is found (i.e. a simulation time from 13s to 133s), due to an increase of approximately 3.5 times for the figure of merit of the FEM model (i.e. degrees of freedom and number of elements). Furthermore the improvement on the estimation of the experimental data derived from a more discretized model is negligible, i.e. the difference is only on the fourth digit of the relative error. This low difference is obtained also in correspondence of the higher temperature, where it is known that the temperature dependency of the HH model itself starts to be less realistic [17]. As a consequence it is possible to assume that also a "soft" discretization of each region is necessary and that a "light" simulation is enough in order to perform a satisfactory study of the phenomenon.

3 Best Numerical Model with Respect to the Objective of the Analysis

In order to study two different problems, we need to select the best numerical model, ensuring the desired analysis without introducing a not necessary hard computational effort. In particular, if we are interested, for example, in the reproduction of the spiking effect due to an increase in temperature or to a study finalized to quantitative interpreting the number of APs or, in the end, to determining the maximum TMV value assumed along the longitudinal extension of the axon, the Model B can be adopted. Whereas, if we are interested on the visualization of the behaviour inside the membrane during AP propagation, and its effect around the external medium, the Model A with membrane can be more conveniently adopted. In the two following subsections the results are reported and some comments are indicated.

3.1 Temperature Dependence of the Firing Effect

A parametric study of the TMV with respect to the temperature is made by performing numerical simulation on the Model B, which leads to the time behaviours depicted in Figure 6.

In particular the range [9-21]°C is considered with a step of 3°C for each case. This picture shows how, as theoretically expected [17], the spiking of the neuron is affected by a change in the temperature. Moreover, it can be observed, in Figure 6 and, particularly, in Fig 6 a and b) (zooming on the first AP) that the maximum value

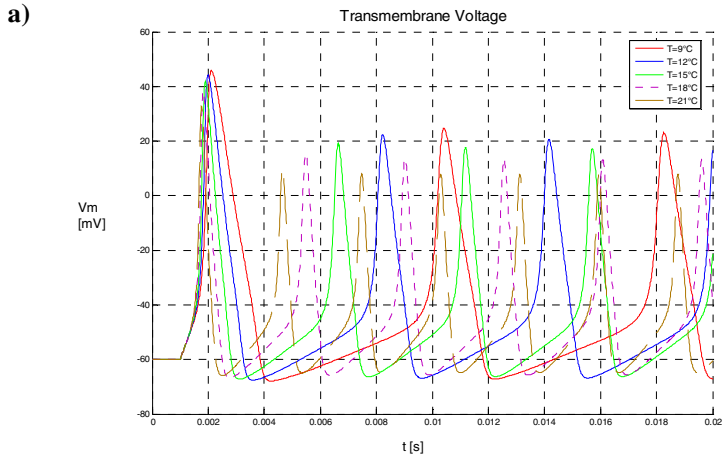

Fig. 6. Temperature dependency of the AP behaviour: a) number of APs in the same time window; b) first AP peak; c) TMV behaviour at a particular temperature (T=18.3°C)

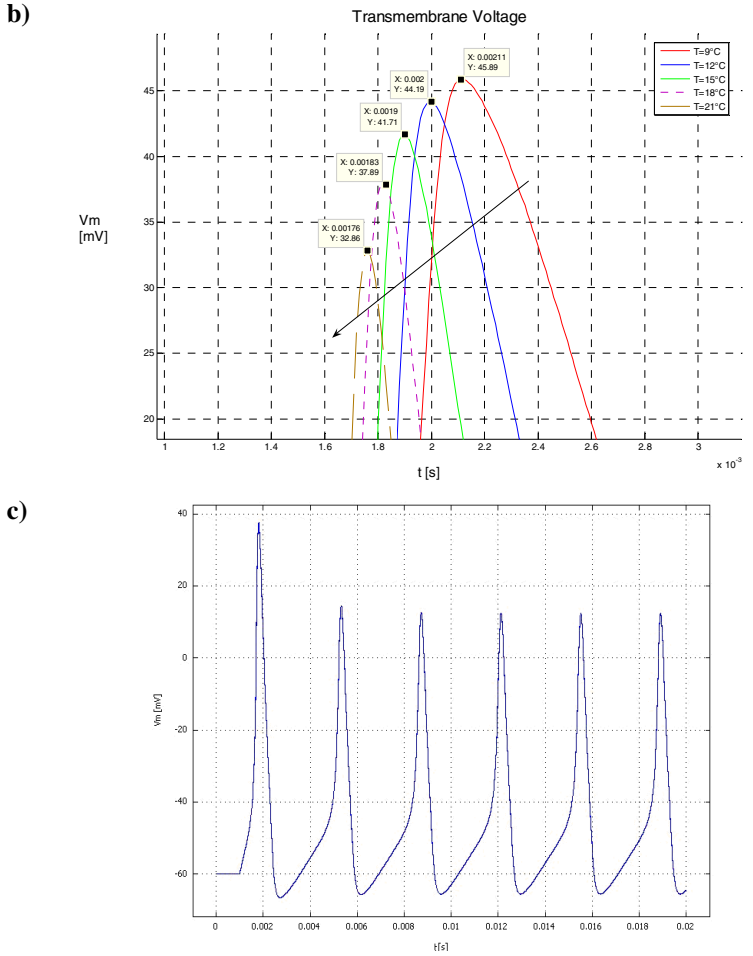

Fig. 6. (*continued*)

assumed by the *Vm(t)* gets lower and lower increasing the value of the ambient temperature, while the duration of the spikes gets minor in contrast with the number of them (three spikes for the case at T=9°C and seven for T=21°C).

In particular, as a particular exemplification case in Fig 5c) we have chosen to show when the temperature assumes a particular value of 18.5°C. In this case the membrane response results in a sequence of six APs, shorter than the two observed at lower temperature reported in Figure 4d). In particular we also check the temperature effects on channels gating process by observing that in turn, channels time constants affect membrane dynamics, which can be represented by the time dependences of the channels conductances ([22]-[23]), reported in Figure 7.

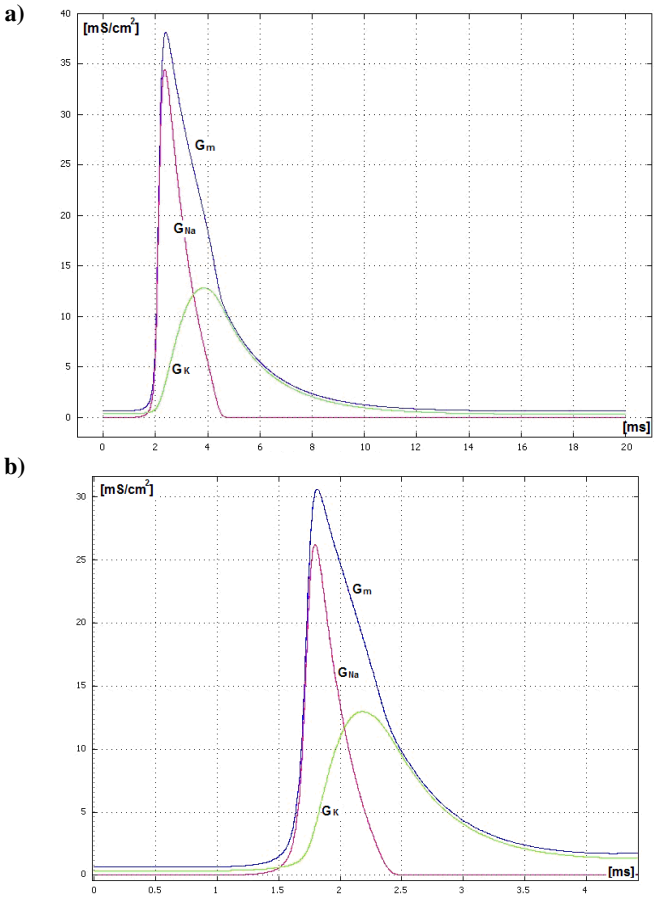

Fig. 7. Temporal dynamic shapes for G_{Na}, G_K, G_l at different temperatures: a) T= 6.3°C; b) T=18.3°C

The maximum of the conductance for each channel is reached faster at higher temperature - case reported in Figure 7b) with T=18.3°C -whereas the duration of the opening of the channel, i.e. a significant value for each conductance, is longer at lower temperature - case depicted in Figure 6a- with T=6.3°C) as confirmed by equation (14).

3.2 The Propagation of the AP along the Membrane Domain

In order to obtain the visualization of the AP propagation inside the membrane, and its effect around the external space, the Model A with membrane is here conveniently adopted. Specifically, in accord to HH experimental setup, once the resting state conditions have been achieved all over the structures, a potential difference, beyond the natural excitement threshold [24], can be fixed across membrane at any transversal section (in this case at z = 0) of the model to elicit a local action potential.

This propagates along the considered axon segment, thanks to the well-known physiological mechanisms of non-myelinated fibres, whose reproduction was the objective of this simulation phase. In particular, this is achieved by fixing a 15mV voltage difference across axon membrane at z=0, thus obtaining the propagation effect shown in Figure 8.

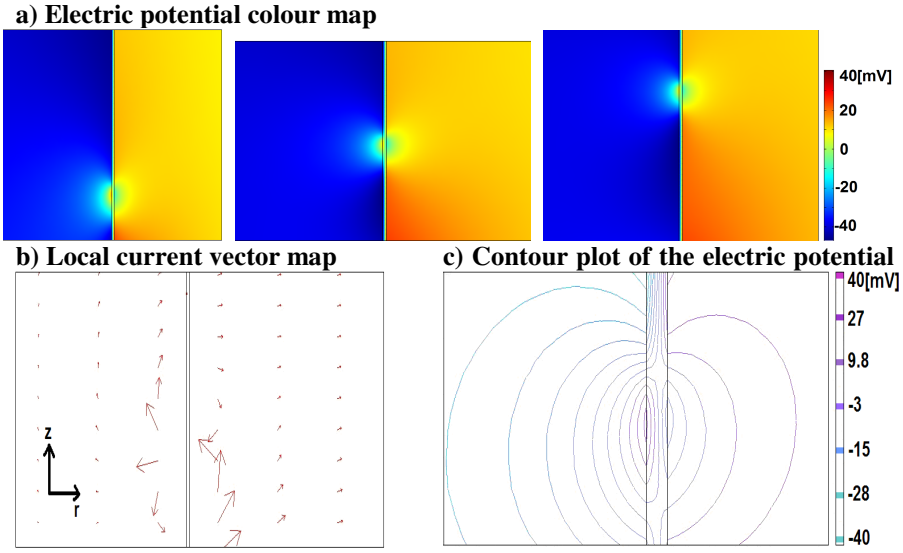

Fig. 8. a) Propagation phenomenon: the moving active zone (z∈ [0.02,0.3]μm and r [0.25,0.75] μm). Potential map at three different times of pulse conduction. **b)** Simulation results for local currents in an activated zone. **c)** Zoom in an active zone: electric potential lines inside and outside membrane (z∈ [0.09, 0.13]μm and r [0.45,0.54] μm).

The explanation of these results is the presence in a certain instant of an AP in an area (the *active zone*, emulated constraining the value of TMV at z=0). This implies that the inner side of the membrane is electrically "more positive" with respect to the outer one. The charge distribution non-homogeneity, thus created, induces longitudinal potential gradients; these in turn generate electric currents (known as *local currents*) in both intra and extra-cellular media, whose lines merge into the active zone (Figure 8b and 8c). All this process results, as expected theoretically, in the activation of the other near areas interested by these charge fluxes. Simulation results for model A are reported to show equipotential lines distribution within an activated section of membrane domain (Figure 8c).

Conclusions and Future Work

It is shown that the two FEM models, here described, allow to simulate the electrophysiological behaviour of a portion of nervous cell axon, to carry out the simulation of the static, underthreshold and active dynamic behaviour, to reproduce

action potentials. The maximum deviation in the prediction of the two models in correspondence of the TMV peak-value has proved to be almost 0.05% with respect to an increase in the computational cost of a factor five. It is also shown that the quality of the FEM discretization is not relevant with respect to the capability of the solution method in order to reproduce the expected behaviour. In particular the capability of the FEM solution to reproduce the temperature dependency of the TMV is investigated leading to assume that also a "soft" discretization of each region is sufficient and that a "light" simulation is enough in order to perform a satisfactory study of the phenomenon. Both the proposed models grant the calculation of the electric potential distribution in the space. The Model A, with the direct representation of the axolemma, is unavoidable if the behaviour of the electromagnetic characteristic inside the membrane is matter of interest, whereas the second coarser one (Model B) is computationally more efficient in all the other cases. Therefore, the AP temperature dependences and the propagation effects are reproduced by using the corresponding "best" numerical models, i.e. the coarse one without membrane for the temperature, the more detailed with membrane for the propagation, leading to a trade off between the computational effort and the objective of the analysis. The models are a very useful starting point for a wide range of future works for different application and extension in order to understand, for example, the true behaviour of a complete neuron. It is now possible, without dealing with enormous form factors, to simulate a whole non-myelinated fibre, to introduce more detailed geometry in the structure such as soma and dendrites, implementing their behaviour simply considering locally differentiated channel densities and translating them into opportune conductances per unit area. Also for this topics opportune considerations on the computational cost must be taken into account: when a lower computation effort is required, the adoption of the Model B can be conveniently considered in order to evaluate phenomena external to the membrane domain, otherwise the "more realistic" Model A should be adopted.

Acknowledgment. The results here presented have been partially shown at the European COMSOL Conference 2009, oct 14-15 2009, Milan, Italy [25].

References

[1] Finn, W., LoPresti, P.: The Handbook of Neuroprosthetic Methods. CRC Press (2003)
[2] Talelea, S., Gaynor, P.: Non-linear time domain model of electropermeabilization: Response of a single cell to an arbitrary applied electric field. Journal of Electrostatics 65, 775–784 (2007)
[3] Koch, C., Segev, I.: Methods in Neuronal Modeling: From Synapses to Networks. MIT Press, Cambridge (1989)
[4] Ying, Z., et al.: Micro-stimulator Design for Visual Prosthesis based on Optic Nerve Stimulation. In: International Symposium on Biophotonics, Nanophotonics and Metamaterials, pp. 139–142 (2006)
[5] Berger, et al.: Brain-Implantable Biomimetic Electronics as Neural Prosthetics. In: Proceedings of the 1st International IEEE EMBS Conference on Neural Engineering, Capri Island, Italy, March 20-22 (2003)

[6] Daniel, J., et al.: Chronic Intraneural Electrical Stimulation For Prosthetic Sensory Feedback. In: Proceedings of the 1st International IEEE EMBS Conference on Neural Engineering, Capri Island, Italy, March 20-22 (2003)
[7] Moulin, C., et al.: A New 3-D Finite-Element Model Based on Thin-Film Approximation for Microelectrode Array Recording of Extracellular Action Potential. IEEE Transactions on Biomedical Engineering 55(2), 683–692 (2008)
[8] Hodgkin, A.L., Huxley, A.F.: A quantitative description of membrane current and its application to conduction and excitation in nerve. J. Physiol. 117, 500–544 (1952)
[9] McIntyre, C.C., Grill, W.M.: Microstimulation of spinal motoneurons: a model study. In: Proceedings of the 19th International Conference - IEEE/EMBS, Chicago, IL, USA, October 30-November 2 (1997)
[10] Woo, J., Miller, C.A., Abbas, P.J.: Biophysical Model of an Auditory Nerve Fiber With a Novel Adaptation Component. IEEE Transactions on Biomedical Engineering 56(9), 2177–2180 (2009)
[11] Greenberg, R.J., Velte, T.J., Humayun, M.S., Scarlatis, G.N., de Juan Jr., E.: A Computational Model of Electrical Stimulation of the Retinal Ganglion Cell. IEEE Transactions on Biomedical Engineering 46(5), 505–514 (1999)
[12] Tupsie, S., Isaramongkolrak, A., Paolaor, P.: Analysis of Electromagnetic Field Effects Using FEM for Transmission Lines Transposition. World Academy of Science, Engineering and Technology 53, 870–874 (2009)
[13] Holt, G.R., Koch, C.: Electrical Interactions via the Extracellular Potential Near Cell Bodies. Journal of Computational Neuroscience 6(2), 169–184 (1999)
[14] Stickler, Y., Martinek, J., Rattay, F.: Modeling Needle Stimulation of Denervated Muscle Fibers: Voltage–Distance Relations and Fiber Polarization Effects. IEEE Transactions on Biomedical Engineering 56(10), 2396–2403 (2009)
[15] Hodgkin, A.L., Katz, B.: The effect of temperature on the electrical activity of the giant axon of the squid. J. Physiol. 109, 240–249 (1949)
[16] Keynes, R.D.: The ionic movements during nervous activity. J. Physiol. 114, 119–150 (1951)
[17] Huxley, A.F.: Ion movements during nerve activity. Annals of the New York Academy of Sciences 81, 221–246 (1959)
[18] COMSOL Multiphysics 3.2 Reference Manual, Thin Film Resistance application example
[19] Izhikevich, E.M.: Which Model to Use for Cortical Spiking Neurons? IEEE Transaction on Neuronal Networks 15(5), 1063–1070 (2004)
[20] Moulin, C.: Contribution à l'étude et à la réalisation d'un système électronique de mesure et excitation de tissu nerveux à matrices de microélectrodes. Thèse Institut National des Sciences Appliquées de Lyon, p. 163 (2006)
[21] Rattay, F.: Electrical Nerve Stimulation: Theory, Experiments and Applications. Springer (August 2001) ISBN: 321182247X
[22] Malmivuo, Plonsey, R.: Bioelectromagnetism. Principles and Applications of Bioelectric and Biomagnetic Fields. Oxford University Press (1995)
[23] Taglietti, Casella, C.: Elementi di fisiologia e biofisica della cellula. La goliardica Pavese Editore, Italy (1997)
[24] Rattay, F.: Analysis of the electrical excitation of CNS neurons. IEEE Transaction on Biomedical Engineering 45(6), 766–772 (1998)
[25] Elia, S., Lamberti, P., Tucci, V.: A Finite Element Model for The Axon of Nervous Cells. In: COMSOL Europe Conference 2009, October 14-16, pp. 1–7 (2009) ISBN/ISSN: 978-0-9825697-0-2